

**Testing Hořava-Lifshitz gravity using thin accretion disk properties**

Tiberiu Harko\* and Zoltán Kovács

*Department of Physics and Center for Theoretical and Computational Physics, The University of Hong Kong, Pok Fu Lam Road, Hong Kong*

Francisco S. N. Lobo†

*Centro de Física Teórica e Computacional, Faculdade de Ciências da Universidade de Lisboa, Avenida Professor Gama Pinto 2, P-1649-003 Lisboa, Portugal*

(Received 8 July 2009; published 24 August 2009)

Recently, a renormalizable gravity theory with higher spatial derivatives in four dimensions was proposed by Hořava. The theory reduces to Einstein gravity with a nonvanishing cosmological constant in IR, but it has improved UV behaviors. The spherically symmetric black hole solutions for an arbitrary cosmological constant, which represent the generalization of the standard Schwarzschild–(anti) de Sitter solution, have also been obtained for the Hořava-Lifshitz theory. The exact asymptotically flat Schwarzschild-type solution of the gravitational field equations in Hořava gravity contains a quadratic increasing term, as well as the square root of a fourth order polynomial in the radial coordinate, and it depends on one arbitrary integration constant. The IR-modified Hořava gravity seems to be consistent with the current observational data, but in order to test its viability more observational constraints are necessary. In the present paper we consider the possibility of observationally testing Hořava gravity by using the accretion disk properties around black holes. The energy flux, the temperature distribution, the emission spectrum, as well as the energy conversion efficiency are obtained, and compared to the standard general relativistic case. Particular signatures can appear in the electromagnetic spectrum, thus leading to the possibility of directly testing Hořava gravity models by using astrophysical observations of the emission spectra from accretion disks.

DOI: [10.1103/PhysRevD.80.044021](https://doi.org/10.1103/PhysRevD.80.044021)

PACS numbers: 04.50.Kd, 04.70.Bw, 97.10.Gz

**I. INTRODUCTION**

Recently, Hořava proposed a renormalizable gravity theory in four dimensions which reduces to Einstein gravity with a nonvanishing cosmological constant in IR but with improved UV behaviors [1,2]. The latter theory admits a Lifshitz scale invariance in time and space, exhibiting a broken Lorentz symmetry at short scales, while at large distances higher derivative terms do not contribute, and the theory reduces to standard general relativity (GR). Since then various properties and characteristics of the Hořava gravities have been extensively analyzed, ranging from formal developments [3], cosmology [4], dark energy [5] and dark matter [6], and spherically symmetric solutions [7–10]. Although a generic vacuum of the theory is an anti-de Sitter (AdS) one, particular limits of the theory allow for the Minkowski vacuum. In this limit post-Newtonian coefficients coincide with those of the pure GR. Thus, the deviations from the conventional GR can be tested only beyond the post-Newtonian corrections, that is for a system with strong gravity at astrophysical scales.

In this context, IR-modified Hořava gravity seems to be consistent with the current observational data, but in order to test its viability more observational constraints are necessary. In Ref. [11], potentially observable properties of

black holes in the Hořava-Lifshitz gravity with Minkowski vacuum were considered, namely, the gravitational lensing and quasinormal modes. It was shown that the bending angle is seemingly smaller in the considered Hořava-Lifshitz gravity than in GR, and the quasinormal modes of black holes are longer lived, and have larger real oscillation frequency in the Hořava-Lifshitz gravity than in GR. In Ref. [12], by adopting the strong field limit approach, the properties of strong field gravitational lensing in the deformed Hořava-Lifshitz black hole were considered, and the angular position and magnification of the relativistic images were obtained. Compared with the Reissner-Nordström black hole, a significant difference in the parameters was found. Thus, it was argued this may offer a way to distinguish a deformed Hořava-Lifshitz black hole from a Reissner-Nordström black hole. In Ref. [13], the behavior of the effective potential was analyzed, and the timelike geodesic motion in the Hořava-Lifshitz spacetime was also explored. In this paper, we further explore the possibility of testing the viability of Hořava-Lifshitz gravity using thin accretion disk properties.

Recent observations suggest that around almost all of the active galactic nuclei, or black hole candidates, there exist gas clouds surrounding the central compact object, together with an associated accretion disk, on a variety of scales from one-tenth of a parsec to a few hundred parsecs [14]. These gas clouds are assumed to form a geometrically and optically thick torus (or warped disk), which absorbs

\*harko@hkuc.hku.hk

†fobo@cii.fis.ul.pt

most of the ultraviolet radiation and the soft x rays. The gas exists in either the molecular or the atomic phase. The most powerful evidence for the existence of super massive black holes comes from the very long baseline interferometry (VLBI) imaging of molecular H<sub>2</sub>O masers in the active galaxy NGC 4258 [15]. This imaging, produced by Doppler shift measurements assuming Keplerian motion of the masing source, has allowed a quite accurate estimation of the central mass, which has been found to be a  $3.6 \times 10^7 M_\odot$  super massive dark object, within 0.13 pc. Hence, important astrophysical information can be obtained from the observation of the motion of the gas streams in the gravitational field of compact objects.

The mass accretion around rotating black holes was studied in general relativity for the first time in [16]. By using an equatorial approximation to the stationary and axisymmetric spacetime of rotating black holes, steady-state thin disk models were constructed, extending the theory of nonrelativistic accretion [17]. In these models hydrodynamical equilibrium is maintained by efficient cooling mechanisms via radiation transport, and the accreting matter has a Keplerian rotation. The radiation emitted by the disk surface was also studied under the assumption that blackbody radiation would emerge from the disk in thermodynamical equilibrium. The radiation properties of the thin accretion disks were further analyzed in [18,19], where the effects of the photon capture by the hole on the spin evolution were presented as well. In these works the efficiency with which black holes convert rest mass into outgoing radiation in the accretion process was also computed.

More recently, the emissivity properties of the accretion disks were investigated for exotic central objects, such as wormholes [20,21], and nonrotating or rotating quark, boson, or fermion stars, brane-world black holes or gravastars [22–28]. The radiation power per unit area, the temperature of the disk, and the spectrum of the emitted radiation were given, and compared with the case of a Schwarzschild black hole of an equal mass. The physical properties of matter forming a thin accretion disk in the static and spherically symmetric spacetime metric of vacuum  $f(R)$  modified gravity models were also analyzed [29]. Particular signatures can appear in the electromagnetic spectrum, thus leading to the possibility of directly testing modified gravity models by using astrophysical observations of the emission spectra from accretion disks.

It is the purpose of the present paper to study the thin accretion disk models applied for black holes in Hořava-Lifshitz gravity models, and carry out an analysis of the properties of the radiation emerging from the surface of the disk. As compared to the standard general relativistic case, significant differences appear in the energy flux and electromagnetic spectrum for Hořava black holes, thus leading to the possibility of directly testing the Hořava-Lifshitz theory by using astrophysical observations of the emission spectra from accretion disks.

This paper is organized as follows. In Sec. II, we present the action and specific solutions of static and spherically symmetric spacetimes. In Sec. III, we review the formalism and the physical properties of the thin disk accretion onto compact objects. In Sec. IV, we analyze the basic properties of matter forming a thin accretion disk around vacuum black holes in Hořava gravity, and compare the results with the Schwarzschild solution. We discuss and conclude our results in Sec. V.

## II. BLACK HOLES IN HOŘAVA GRAVITY

In this section, we briefly review the Hořava-Lifshitz theory, where differential geometry of foliations represents the proper mathematical setting for the class of gravity theories studied by Hořava [2]. As foliations can be equipped with a Riemannian structure, the dynamical variables in Hořava-Lifshitz gravity is the lapse function  $N$ , the shift vector  $N^i$ , and the three-dimensional spatial metric  $g_{ij}$ . Thus, it is useful to use the Arnowitt-Deser-Misner formalism, where the four-dimensional metric is parametrized by the following:

$$ds^2 = -N^2 c^2 dt^2 + g_{ij}(dx^i + N^i dt)(dx^j + N^j dt). \quad (1)$$

In this context, the Einstein-Hilbert action is given by

$$S = \frac{1}{16\pi G} \int d^4x \sqrt{g} N (K_{ij} K^{ij} - K^2 + R^{(3)} - 2\Lambda), \quad (2)$$

where  $G$  is Newton's constant, and  $R^{(3)}$  is the three-dimensional curvature scalar for  $g_{ij}$ . The extrinsic curvature,  $K_{ij}$ , is defined as

$$K_{ij} = \frac{1}{2N} (\dot{g}_{ij} - \nabla_i N_j - \nabla_j N_i), \quad (3)$$

where the dot denotes a derivative with respect to  $t$ , and  $\nabla_i$  is the covariant derivative with respect to the spatial metric  $g_{ij}$ .

The IR-modified Hořava action is given by

$$\begin{aligned} S = \int dt d^3x \sqrt{g} N & \left[ \frac{2}{\kappa^2} (K_{ij} K^{ij} - \lambda K^2) - \frac{\kappa^2}{2\nu^4} C_{ij} C^{ij} \right. \\ & + \frac{\kappa^2 \mu}{2\nu^2} \epsilon^{ijk} R_{il}^{(3)} \nabla_j R_k^{(3)l} - \frac{\kappa^2 \mu^2}{8} R_{ij}^{(3)} R^{(3)ij} \\ & + \frac{\kappa^2 \mu^2}{8(3\lambda - 1)} \left( \frac{4\lambda - 1}{4} (R^{(3)})^2 - \Lambda_w R^{(3)} + 3\Lambda_w^2 \right) \\ & \left. + \frac{\kappa^2 \mu^2 \omega}{8(3\lambda - 1)} R^{(3)} \right], \quad (4) \end{aligned}$$

where  $\kappa$ ,  $\lambda$ ,  $\nu$ ,  $\mu$ ,  $\omega$ , and  $\Lambda_w$  are constant parameters.  $C^{ij}$  is the Cotton tensor, defined as

$$C^{ij} = \epsilon^{ikl} \nabla_k (R_l^{(3)j} - \frac{1}{4} R^{(3)} \delta_l^j). \quad (5)$$

Note that the last term in Eq. (4) represents a “soft” violation of the “detailed balance” condition, which modi-

fies the IR behavior. This IR modification term,  $\mu^4 R^{(3)}$ , generalizes the original Hořava model (we have used the notation of Ref. [8]). Note that now these solutions with an arbitrary cosmological constant represent the analogs of the standard Schwarzschild–(A)dS solutions, which were absent in the original Hořava model [8].

The fundamental constants of the speed of light  $c$ , Newton's constant  $G$ , and the cosmological constant  $\Lambda$  are defined as

$$c^2 = \frac{\kappa^2 \mu^2 |\lambda_W|}{8(3\lambda - 1)^2}, \quad G = \frac{\kappa^2 c^2}{16\pi(3\lambda - 1)}, \quad (6)$$

$$\Lambda = \frac{3}{2} \Lambda_W c^2.$$

Throughout this work, we consider the static and spherically symmetric metric given by

$$ds^2 = -N^2(r)dt^2 + \frac{dr^2}{f(r)} + r^2(d\theta^2 + \sin^2\theta d\phi^2), \quad (7)$$

where  $N(r)$  and  $f(r)$  are arbitrary functions of the radial coordinate,  $r$ .

Imposing the specific case of  $\lambda = 1$ , which reduces to the Einstein-Hilbert action in the IR limit, one obtains the following solution of the vacuum field equations in Hořava gravity:

$$N^2 = f = 1 + (\omega - \Lambda_W)r^2 - \sqrt{r[\omega(\omega - 2\Lambda_W)r^3 + \beta]}, \quad (8)$$

where  $\beta$  is an integration constant [8].

By considering  $\beta = -\alpha^2/\Lambda_W$  and  $\omega = 0$  the solution given by Eq. (8) reduces to the Lu, Mei, and Pope solution [9], given by

$$f = 1 - \Lambda_W r^2 - \frac{\alpha}{\sqrt{-\Lambda_W}} \sqrt{r}. \quad (9)$$

Alternatively, considering now  $\beta = 4\omega M$  and  $\Lambda_W = 0$ , one obtains the Kehagias and Sfetsos's (KS) asymptotically flat solution [10], given by

$$f = 1 + \omega r^2 - \sqrt{r(\omega^2 r^3 + 4\omega M)}, \quad (10)$$

which is the only asymptotically flat solution in the family of solutions (8). We shall use the Kehagias-Sfetsos solution for analyzing the accretion disk properties. Note that there is an outer (event) horizon, and an inner (Cauchy) horizon at

$$r_{\pm} = M[1 \pm \sqrt{1 - 1/(2\omega M^2)}]. \quad (11)$$

To avoid a naked singularity at the origin, one also needs to impose the condition

$$\omega M^2 \geq \frac{1}{2}. \quad (12)$$

Note that in the GR regime, i.e.,  $\omega M^2 \gg 1$ , the outer

horizon approaches the Schwarzschild horizon,  $r_+ \simeq 2M$ , and the inner horizon approaches the central singularity,  $r_- \simeq 0$ .

### III. ELECTROMAGNETIC RADIATION PROPERTIES OF THIN ACCRETION DISKS

To set the stage, we present the general formalism of electromagnetic radiation properties of thin accretion disks in a general static, spherically symmetric spacetime.

#### A. Spacetime metric and geodesic equations

In this work we analyze the physical properties and characteristics of particles moving in circular orbits around general relativistic compact spheres in a static and spherically symmetric geometry given by the following metric:

$$ds^2 = g_{tt}dt^2 + g_{rr}dr^2 + g_{\theta\theta}d\theta^2 + g_{\phi\phi}d\phi^2. \quad (13)$$

Here the metric components  $g_{tt}$ ,  $g_{rr}$ ,  $g_{\theta\theta}$ , and  $g_{\phi\phi}$  depend only on the radial coordinate  $r$ . In a static and spherically symmetric spacetime two constants of motion for particles do exist, the specific energy  $\tilde{E}$  and of the specific angular momentum  $\tilde{L}$ , respectively. The geodesic equations of motion in the equatorial plane ( $\theta = \pi/2$ ) can be written in terms of these constants of motion as

$$g_{tt}\dot{t} = -\tilde{E}, \quad (14)$$

$$g_{\phi\phi}\dot{\phi} = \tilde{L}, \quad (15)$$

$$-g_{tt}g_{rr}\dot{r}^2 + V_{\text{eff}}(r) = \tilde{E}^2, \quad (16)$$

where the effective potential term is defined as

$$V_{\text{eff}}(r) = -g_{tt}\left(1 + \frac{\tilde{L}^2}{g_{\phi\phi}}\right). \quad (17)$$

For stable circular orbits in the equatorial plane the following conditions must hold:  $V_{\text{eff}}(r) = 0$  and  $V_{\text{eff},r}(r) = 0$ , respectively. These conditions provide the specific energy, the specific angular momentum, and the angular velocity  $\Omega$  of particles moving in circular orbits for the case of static general relativistic compact spheres, given by

$$\tilde{E} = -\frac{g_{tt}}{\sqrt{-g_{tt} - g_{\phi\phi}\Omega^2}}, \quad (18)$$

$$\tilde{L} = \frac{g_{\phi\phi}\Omega}{\sqrt{-g_{tt} - g_{\phi\phi}\Omega^2}}, \quad (19)$$

$$\Omega = \frac{d\phi}{dt} = \sqrt{\frac{-g_{tt,r}}{g_{\phi\phi,r}}}. \quad (20)$$

The marginally stable orbit around the central object can be determined from the condition  $V_{\text{eff},rr}(r) = 0$ . This con-

dition provides the following relation:

$$\tilde{E}^2 g_{\phi\phi,rr} + \tilde{L}^2 g_{tt,rr} + (g_{tt} g_{\phi\phi})_{,rr} = 0. \quad (21)$$

By inserting Eqs. (18)–(20) into Eq. (21), and solving this equation for  $r$ , we obtain the marginally stable orbit for the explicitly given metric coefficients  $g_{tt}$ ,  $g_{t\phi}$ , and  $g_{\phi\phi}$ . For a Schwarzschild black hole we have  $g_{tt} = -(1 - 2M/r)$ ,  $g_{rr} = -g_{tt}^{-1}$ , and  $g_{\phi\phi} = r^2$ , and the geodesic equation (16) for the radial coordinate  $r$  becomes

$$\dot{r}^2 + V_{\text{eff}}(r) = \tilde{E}^2 \quad (22)$$

with the effective potential given by

$$V_{\text{eff}}(r) = \left(1 - \frac{2M}{r}\right) \left(1 + \frac{\tilde{L}^2}{r^2}\right). \quad (23)$$

Equations (18)–(20) lead to the form

$$\tilde{E} = \frac{r(r - 2M)}{\sqrt{r - 3M}}, \quad (24)$$

$$\tilde{L} = \frac{R^5 \Omega}{\sqrt{r - 3M}}, \quad (25)$$

$$\Omega = \sqrt{\frac{M}{r^3}}, \quad (26)$$

for the specific energy, the specific angular momentum, and the angular velocity for the Schwarzschild metric. Since for the KS solution, given by Eq. (10),  $g_{tt} = -f(r)$ ,  $g_{rr} = -g_{tt}^{-1}$ , and  $g_{\phi\phi} = r^2$ , the effective potential in Hořava-Lifshitz theory can be written as

$$V_{\text{eff}}(r) = \left[1 + \omega r^2 - f_{M,\omega}(r)\right] \left(1 + \frac{\tilde{L}^2}{r^2}\right), \quad (27)$$

with  $f_{M,\omega}(r) \equiv \sqrt{r\omega(\omega r^3 + 4M)}$ , whereas the specific energy, the specific angular momentum, and the angular velocity are given by

$$\tilde{E} = \frac{\sqrt{1 + r^2 \omega - f_{M,\omega}}}{\sqrt{1 + r^2(\omega - \Omega^2) - f_{M,\omega}}}, \quad (28)$$

$$\tilde{L} = \frac{r^2 \Omega}{\sqrt{1 + r^2(\omega - \Omega^2) - f_{M,\omega}}}, \quad (29)$$

$$\Omega = \sqrt{\frac{r f_{M,\omega} - M - \omega r^3}{r \sqrt{f_{M,\omega}}}}. \quad (30)$$

The effective potentials of the Schwarzschild black hole and of the KS solution are compared for the same geometrical mass in Fig. 1. As previously shown in [11],  $V_{\text{eff}}(r)$  for the KS solution approaches the Schwarzschild potential for increasing values of  $\omega$ .

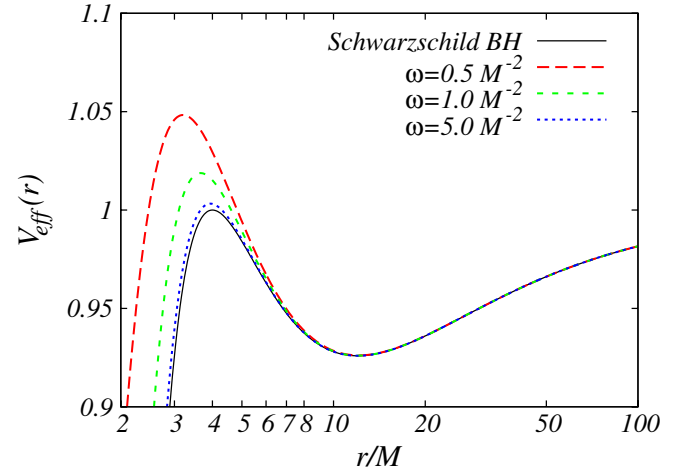


FIG. 1 (color online). The effective potential  $V_{\text{eff}}(r)$  of the orbiting particles for the Kehagias-Sfetsos solution and for the Schwarzschild black hole with the same total mass  $M$  for the specific angular momentum  $\tilde{L} = 4M$ . The parameter  $\omega$  of the Kehagias-Sfetsos solution is set to  $0.5M^{-2}$ ,  $1M^{-2}$ , and  $5M^{-2}$ , respectively.

## B. Properties of thin accretion disks

For a thin accretion disk we assume that its vertical size is negligible, as compared to its horizontal extension, i.e., the disk height  $H$ , defined by the maximum half thickness of the disk, is always much smaller than the characteristic radius  $r$  of the disk,  $H \ll r$ . The thin disk is in hydrodynamical equilibrium, and the pressure gradient and a vertical entropy gradient in the accreting matter are negligible. The efficient cooling via the radiation over the disk surface prevents the disk from cumulating the heat generated by stresses and dynamical friction. In turn, this equilibrium causes the disk to stabilize its thin vertical size. The thin disk has an inner edge at the marginally stable orbit of the compact object potential, and the accreting plasma has a Keplerian motion in higher orbits.

In steady-state accretion disk models, the mass accretion rate  $\dot{M}_0$  is assumed to be a constant that does not change with time. The physical quantities describing the orbiting plasma are averaged over a characteristic time scale, e.g.,  $\Delta t$ , over the azimuthal angle  $\Delta\phi = 2\pi$  for a total period of the orbits, and over the height  $H$  [16–18]. In the standard accretion disk theory the integration of the total divergence of the energy-momentum tensor of the plasma forming the disk provides the disk structure equations. The radiation flux  $F$  emitted by the surface of the accretion disk can be derived from the conservation equations for the mass, energy, and angular momentum, respectively, and it is expressed in terms of the specific energy, angular momentum, and of the angular velocity of the particles orbiting in the disk as [16,18]

$$F(r) = -\frac{\dot{M}_0}{4\pi\sqrt{-g}} \frac{\Omega_{,r}}{(\tilde{E} - \Omega\tilde{L})^2} \int_{r_{\text{ms}}}^r (\tilde{E} - \Omega\tilde{L})\tilde{L}_{,r} dr, \quad (31)$$



where  $\dot{M}_0$  is the mass accretion rate, measuring the rate at which the rest mass of the particles flows inward through the disk with respect to the coordinate time  $t$ , and  $r_{\text{ms}}$  is the marginally stable orbit obtained from Eq. (21), respectively.

Another important characteristic of the mass accretion process is the efficiency with which the central object converts rest mass into outgoing radiation. This quantity is defined as the ratio of the rate of the radiation of energy of photons escaping from the disk surface to infinity, and the rate at which mass energy is transported to the central compact general relativistic object, both measured at infinity [16,18]. If all the emitted photons can escape to infinity, the efficiency is given in terms of the specific energy measured at the marginally stable orbit  $r_{\text{ms}}$ ,

$$\epsilon = 1 - \tilde{E}_{\text{ms}}, \quad (32)$$

For Schwarzschild black holes the efficiency is about 6%, whether the photon capture by the black hole is considered, or not. Ignoring the capture of radiation by the hole,  $\epsilon$  is found to be 42% for extremely rotating Kerr black holes ( $a_* = 1$ ), whereas with photon capture the efficiency is 40% [19].

The accreting matter in the steady-state thin disk model is supposed to be in thermodynamical equilibrium. Therefore the radiation emitted by the disk surface can be considered as a perfect blackbody radiation, where the energy flux is given by  $F(r) = \sigma T^4(r)$  ( $\sigma$  is the Stefan-Boltzmann constant), and the observed luminosity  $L(\nu)$  has a redshifted blackbody spectrum [24]:

$$L(\nu) = 4\pi d^2 I(\nu) = \frac{8}{\pi c^2} \cos\gamma \int_{r_i}^{r_f} \int_0^{2\pi} \frac{\nu_e^3 r d\phi dr}{\exp(h\nu_e/T) - 1}. \quad (33)$$

Here  $d$  is the distance to the source,  $I(\nu)$  is the thermal energy flux radiated by the disk,  $\gamma$  is the disk inclination angle, and  $r_i$  and  $r_f$  indicate the position of the inner and outer edge of the disk, respectively. We take  $r_i = r_{\text{ms}}$  and  $r_f \rightarrow \infty$ , since we expect the flux over the disk surface vanishes at  $r \rightarrow \infty$  for any kind of asymptotically flat geometry. The emitted frequency is given by  $\nu_e = \nu(1+z)$ , where the redshift factor can be written as

$$1+z = \frac{1 + \Omega r \sin\phi \sin\gamma}{\sqrt{-g_{tt} - 2\Omega g_{t\phi} - \Omega^2 g_{\phi\phi}}}, \quad (34)$$

where we have neglected the light bending [30,31].

#### IV. ELECTROMAGNETIC SIGNATURES OF ACCRETION DISKS AROUND KEHAGIAS-SFETSOS BLACK HOLES

As a first step in the study of the accretion disk properties, we obtain Eqs. (28)–(30) for the specific energy  $\tilde{E}$ , the specific angular momentum  $\tilde{L}$ , and the angular velocity  $\Omega$

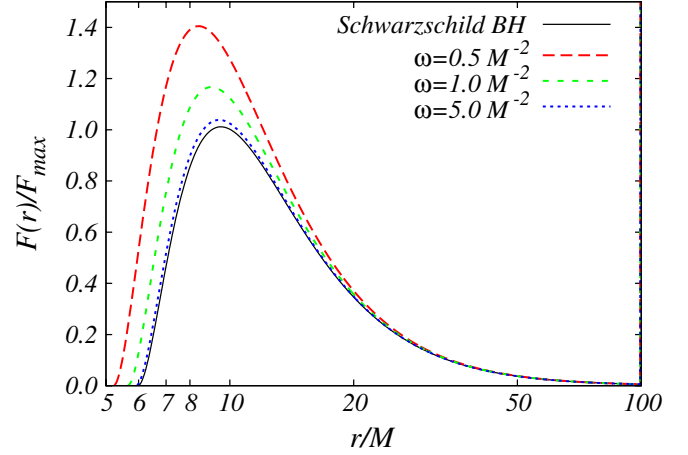


FIG. 2 (color online). The energy radiated by a disk around the Kehagias-Sfetsos and Schwarzschild black holes with the same total mass  $M$ . The parameter  $\omega$  of the Kehagias-Sfetsos solution is set to  $0.5M^{-2}$ ,  $1M^{-2}$ , and  $5M^{-2}$ , respectively, and the flux values are normalized by  $F_{\text{max}} = 1.37 \times 10^{-5} \dot{M}_0/M^2$ , the maximal flux value for the Schwarzschild black hole.

of any particle orbiting around a KS black hole. By inserting Eqs. (28)–(30) into the flux integral Eq. (31), we can derive the radial profile of the emitted photon energy flux over the whole surface of the disk in the KS potential. Equation (31) is derived by integrating the conservation laws for the mass, energy, and angular momentum, which are invariant for Hořava gravity, since the extra terms in the action Eq. (4) do not give any contribution to the total divergence of the stress energy tensor.

The profiles for the energy flux are presented, for different values of  $\omega$ , in Fig. 2. For the sake of comparison we also present the flux distribution over a disk rotating around a Schwarzschild black hole.

Similar to the case of the effective potential, the deviation of  $F(r)$  for the KS geometry from the standard Schwarzschild flux increases as  $\omega$  tends to  $0.5M^{-2}$ . The left edge of the flux profiles, shifting from  $r/M = 6$  to lower radii, shows that the distance of the inner edge of the accretion disk and the event horizon of the KS black hole remains almost the same as for the Schwarzschild geometry (see Table I). For  $\omega = 0.5M^{-2}$  the degenerate event horizon of the KS black hole is at  $r = M$ , and the marginally stable orbit approaches  $r/M = 5$ . The maximal flux

TABLE I. The marginally stable orbit and the efficiency for Kehagias-Sfetsos and Schwarzschild black hole geometries. The last line corresponds to the standard general relativistic Schwarzschild black hole.

$\omega [M^{-2}]$	$r_{\text{ms}} [M]$	$\epsilon$
0.5	5.2441	0.0630
1.0	5.6644	0.0597
5.0	5.9536	0.0576
...	6.0000	0.0572

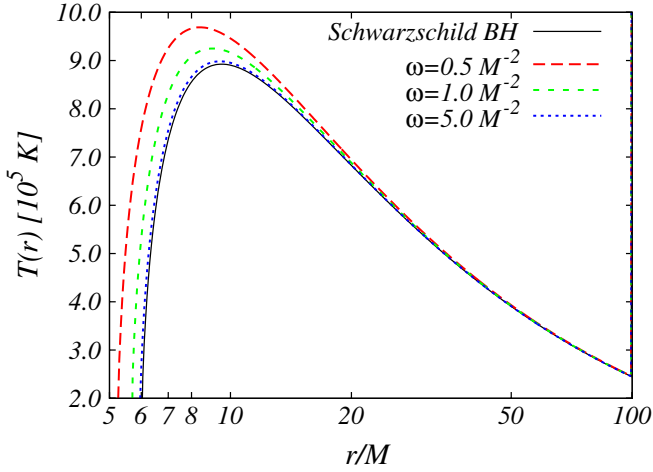


FIG. 3 (color online). The disk temperature for Kehagias-Sfetsos and Schwarzschild black holes with the same total mass  $M$ . The parameter  $\omega$  of the Kehagias-Sfetsos solution is set to  $0.5M^{-2}$ ,  $1M^{-2}$ , and  $5M^{-2}$ , respectively.

value also increases for smaller values of  $\omega$ . When  $\omega M^2$  reaches its lower limit at 0.5, the maximum value of the flux is already a factor of 1.4 higher than the maximum value  $F_{\max} = 1.37 \times 10^{-5} \dot{M}_0/M^2$  corresponding to the Schwarzschild solution. Similar to the inner edge of the disk, the flux maximum is shifted to lower and lower radii by decreasing  $\omega$ .

These features can also be observed in the temperature profiles presented in Fig. 3. However, the differences in the temperature amplitudes are not so big as they are in the case of the flux distribution.

In Fig. 4, the spectral energy distribution, calculated with the use of Eqs. (33) and (34), respectively, shows a more interesting difference between the disk spectra of the KS black hole and of the Schwarzschild black hole, re-

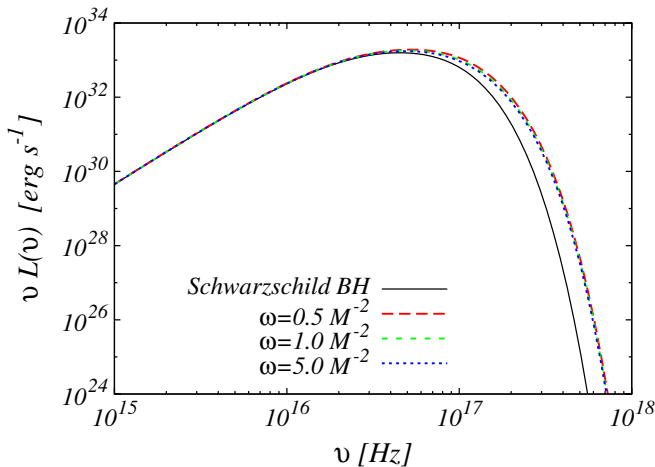


FIG. 4 (color online). Disk spectra for Kehagias-Sfetsos and Schwarzschild black holes with the same total mass  $M$ . The parameter  $\omega$  of the Kehagias-Sfetsos solution is set to  $0.5M^{-2}$ ,  $1M^{-2}$ , and  $5M^{-2}$ , respectively. Here  $M = 1M_\odot$  and  $\dot{M}_0 = 10^{-12}M_\odot/\text{yr}$ .

spectively. The disk spectra are very similar for both the KS and the Schwarzschild black holes in the region with  $\nu \leq 10^{16}$  Hz. The cutoff frequencies of the spectra are also of the order of  $\approx 10^{16}$  Hz for all cases, but they are somewhat higher for the KS black holes than for the Schwarzschild case, which separates the two classes. For the KS solution the spectral properties do not exhibit any significant differences with the variation of  $\omega$ : the spectra are essentially the same for any value of  $\omega$ . Although the amplitude and the cutoff frequency of the spectra are maximal in the limit  $\omega = 0.5M^{-2}$ , the differences in these quantities are negligible even for  $\omega = 1000M^{-2}$ .

Table I shows the conversion efficiency  $\epsilon$  of the accreted mass into radiation for both KS and Schwarzschild black holes. For a given configuration with a fixed value of  $\omega$ ,  $\epsilon$  is somewhat higher in the accretion process driven by KS black holes, as compared to the Schwarzschild geometry. This means that KS black holes always convert more efficiently mass into radiation than a standard general relativistic, static black hole does. The most efficient mechanism is provided by the KS black holes for the minimal value of  $\omega$ , where efficiency is 6.3%. For  $\omega M^2 \gg 1$ , the values of  $\epsilon$  and  $r_{\text{ms}}$  approach those of the Schwarzschild black hole, as expected.

## V. DISCUSSIONS AND FINAL REMARKS

In the present paper we have considered the basic physical properties of matter forming a thin accretion disk in the vacuum spacetime metric of the Hořava-Lifshitz gravity models. The physical parameters of the disk—effective potential, flux, and emission spectrum profiles—have been explicitly obtained for several values of the parameter  $\omega$  characterizing the vacuum solution of the generalized field equations. All the astrophysical quantities, related to the observable properties of the accretion disk, can be obtained from the black hole metric. Because of the differences in the spacetime structure, the Hořava-Lifshitz theory black holes present some very important differences with respect to the disk properties, as compared to the standard general relativistic Schwarzschild case.

The determination of the accretion rate for an astrophysical object can give strong evidence for the existence of a surface of the object. A model in which Sgr A\*, the  $3.7 \times 10^6 M_\odot$  super massive black hole candidate at the Galactic center, may be a compact object with a thermally emitting surface was considered in [32]. For very compact surfaces within the photon orbit, the thermal assumption is likely to be a good approximation because of the large number of rays that are strongly gravitationally lensed back onto the surface. Given the very low quiescent luminosity of Sgr A\* in the near infrared, the existence of a hard surface, even in the limit in which the radius approaches the horizon, places a severe constraint on the steady mass accretion rate onto the source,  $\dot{M} \leq 10^{-12} M_\odot \text{ yr}^{-1}$ . This limit is well below the minimum accretion rate needed to power the observed

submillimeter luminosity of Sgr A\*,  $\dot{M} \geq 10^{-10} M_{\odot} \text{ yr}^{-1}$ . Thus, from the determination of the accretion rate it follows that Sgr A\* does not have a surface, that is, it must have an event horizon.

Therefore, the study of the accretion processes by compact objects is a powerful indicator of their physical nature. Since the energy flux, the temperature distribution of the disk, the spectrum of the emitted blackbody radiation, as well as the conversion efficiency show, in the case of the Hořava-Lifshitz theory vacuum solutions, significant differences as compared to the general relativistic case, the

determination of these observational quantities could discriminate, at least in principle, between standard general relativity and Hořava-Lifshitz theory, and constrain the parameter of the model.

## ACKNOWLEDGMENTS

The work of T.H. was supported by the General Research Fund Grant No. HKU 701808P of the government of the Hong Kong Special Administrative Region.

- 
- [1] P. Horava, J. High Energy Phys. 03 (2009) 020.  
 [2] P. Horava, Phys. Rev. D **79**, 084008 (2009).  
 [3] T.P. Sotiriou, M. Visser, and S. Weinfurter, Phys. Rev. Lett. **102**, 251601 (2009); M. Visser, Phys. Rev. D **80**, 025011 (2009); P. Horava, Phys. Rev. Lett. **102**, 161301 (2009); R. G. Cai, Y. Liu, and Y. W. Sun, J. High Energy Phys. 06 (2009) 010; B. Chen and Q. G. Huang, arXiv:0904.4565; D. Orlando and S. Reffert, Classical Quantum Gravity **26**, 155021 (2009); R. G. Cai, B. Hu, and H. B. Zhang, arXiv:0905.0255; T. Nishioka, arXiv:0905.0473; M. Li and Y. Pang, J. High Energy Phys. 08 (2009) 015; C. Charmousis, G. Niz, A. Padilla, and P. M. Saffin, arXiv:0905.2579; T. P. Sotiriou, M. Visser, and S. Weinfurter, arXiv:0905.2798; G. Calcagni, arXiv:0905.3740; D. Blas, O. Pujolas, and S. Sibiryakov, arXiv:0906.3046; R. Iengo, J. G. Russo, and M. Serone, arXiv:0906.3477; C. Germani, A. Kehagias, and K. Sfetsos, arXiv:0906.1201; S. Mukohyama, arXiv:0906.5069; A. Kobakhidze, arXiv:0906.5401.  
 [4] T. Takahashi and J. Soda, Phys. Rev. Lett. **102**, 231301 (2009); G. Calcagni, arXiv:0904.0829; E. Kiritsis and G. Kofinas, arXiv:0904.1334; S. Mukohyama, J. Cosmol. Astropart. Phys. 06 (2009) 001; R. Brandenberger, arXiv:0904.2835; Y. S. Piao, arXiv:0904.4117; X. Gao, arXiv:0904.4187; S. Mukohyama, K. Nakayama, F. Takahashi, and S. Yokoyama, arXiv:0905.0055; T. Ha, Y. Huang, Q. Ma, K. D. Pechan, T. J. Renner, Z. Wu, and A. Wang, arXiv:0905.0396; S. Kalyana Rama, Phys. Rev. D **79**, 124031 (2009); B. Chen, S. Pi, and J. Z. Tang, arXiv:0905.2300; X. Gao, Y. Wang, R. Brandenberger, and A. Riotto, arXiv:0905.3821; M. Minamitsuji, arXiv:0905.3892; A. Wang and Y. Wu, J. Cosmol. Astropart. Phys. 07 (2009) 012; S. Nojiri and S. D. Odintsov, arXiv:0905.4213; Y. F. Cai and E. N. Saridakis, arXiv:0906.1789.  
 [5] E. N. Saridakis, arXiv:0905.3532; M. i. Park, arXiv:0906.4275.  
 [6] S. Mukohyama, arXiv:0905.3563.  
 [7] H. Nastase, arXiv:0904.3604; R. G. Cai, L. M. Cao, and N. Ohta, Phys. Rev. D **80**, 024003 (2009); Y. S. Myung and Y. W. Kim, arXiv:0905.0179; R. G. Cai, L. M. Cao, and N. Ohta, arXiv:0905.0751; R. B. Mann, J. High Energy Phys. 06 (2009) 075; S. Chen and J. Jing, arXiv:0905.1409; M. Botta-Cantcheff, N. Grandi, and M. Sturla, arXiv:0906.0582; A. Castillo and A. Larranaga, arXiv:0906.4380; J. J. Peng and S. Q. Wu, arXiv:0906.5121; E. O. Colgain and H. Yavartanoo, arXiv:0904.4357.  
 [8] M. i. Park, arXiv:0905.4480.  
 [9] H. Lu, J. Mei, and C. N. Pope, arXiv:0904.1595.  
 [10] A. Kehagias and K. Sfetsos, Phys. Lett. B **678**, 123 (2009).  
 [11] R. A. Konoplya, arXiv:0905.1523.  
 [12] S. Chen and J. Jing, Phys. Rev. D **80**, 024036 (2009).  
 [13] J. Chen and Y. Wang, arXiv:0905.2786.  
 [14] C. M. Urry and P. Padovani, Publ. Astron. Soc. Pac. **107**, 803 (1995).  
 [15] M. Miyoshi, J. Moran, J. Herrnstein, L. Greenhill, N. Nakai, P. Diamond, and M. Inoue, Nature (London) **373**, 127 (1995).  
 [16] I. D. Novikov and K. S. Thorne, in *Black Holes*, edited by C. DeWitt and B. DeWitt (Gordon and Breach, New York, 1973).  
 [17] N. I. Shakura and R. A. Sunyaev, Astron. Astrophys. **24**, 33 (1973).  
 [18] D. N. Page and K. S. Thorne, Astrophys. J. **191**, 499 (1974).  
 [19] K. S. Thorne, Astrophys. J. **191**, 507 (1974).  
 [20] T. Harko, Z. Kovacs, and F. S. N. Lobo, Phys. Rev. D **78**, 084005 (2008).  
 [21] T. Harko, Z. Kovacs, and F. S. N. Lobo, Phys. Rev. D **79**, 064001 (2009).  
 [22] S. Bhattacharyya, A. V. Thampan, and I. Bombaci, Astron. Astrophys. **372**, 925 (2001).  
 [23] Z. Kovacs, K. S. Cheng, and T. Harko, Astron. Astrophys. **500**, 621 (2009).  
 [24] D. Torres, Nucl. Phys. **B626**, 377 (2002).  
 [25] Y. F. Yuan, R. Narayan, and M. J. Rees, Astrophys. J. **606**, 1112 (2004).  
 [26] F. S. Guzman, Phys. Rev. D **73**, 021501 (2006).  
 [27] C. S. J. Pun, Z. Kovacs, and T. Harko, Phys. Rev. D **78**, 084015 (2008).  
 [28] T. Harko, Z. Kovacs, and F. S. N. Lobo, arXiv:0905.1355.  
 [29] C. S. J. Pun, Z. Kovacs, and T. Harko, Phys. Rev. D **78**, 024043 (2008).  
 [30] J. P. Luminet, Astron. Astrophys. **75**, 228 (1979).  
 [31] S. Bhattacharyya, R. Misra and A. V. Thampan, Astrophys. J. **550**, 841 (2001).  
 [32] A. E. Broderick and R. Narayan, Astrophys. J. Lett. **636**, L109 (2006).